STEM CELLS®

CANCER STEM CELLS

Inhibition of Ataxia Telangiectasia- and Rad3-Related Function Abrogates the In Vitro and In Vivo Tumorigenicity of Human Colon Cancer Cells Through Depletion of the CD133$^+$ Tumor-Initiating Cell Fraction

EIKE GALLMEIER,[a] PATRICK C. HERMANN,[b] MARIA-THERESA MUELLER,[b] JUAN G. MACHADO,[b] ANDREAS ZIESCH,[a] ENRICO N. DE TONI,[a] ANDREAS PALAGYI,[a] CHRISTIAN EISEN,[c] JOACHIM W. ELLWART,[d] JOSE RIVERA,[b] BELEN RUBIO-VIQUEIRA,[b] MANUEL HIDALGO,[b] FRED BUNZ,[e] BURKHARD GÖKE,[a] CHRISTOPHER HEESCHEN[b]

[a]Department of Medicine II, Campus Grosshadern, Ludwigs-Maximilian-University of Munich, Munich, Germany; [b]Clinical Research Programme, Spanish National Cancer Research Centre (CNIO), Madrid, Spain; [c]Division of Stem Cells and Cancer, German Cancer Research Centre (DKFZ), Heidelberg, Germany; [d]Institute of Molecular Immunology, Helmholtz Centre, Munich, Germany; [e]Department of Radiation Oncology at Johns Hopkins University, Baltimore, Maryland, USA

Key Words. ATR • Cancer stem cells • Colon cancer • DNA-damage response • Tumor-initiating cells

ABSTRACT

The identification of novel approaches to specifically target the DNA-damage checkpoint response in chemotherapy-resistant cancer stem cells (CSC) of solid tumors has recently attracted great interest. We show here in colon cancer cell lines and primary colon cancer cells that inhibition of checkpoint-modulating phosphoinositide 3-kinase-related (PIK) kinases preferentially depletes the chemoresistant and exclusively tumorigenic CD133$^+$ cell fraction. We observed a time- and dose-dependent disproportionally pronounced loss of CD133$^+$ cells and the consecutive lack of in vitro and in vivo tumorigenicity of the remaining cells. Depletion of CD133$^+$ cells was initiated through apoptosis of cycling CD133$^+$ cells and further substantiated through subsequent recruitment of quiescent CD133$^+$ cells into the cell cycle followed by their elimination. Models using specific PIK kinase inhibitors, somatic cell gene targeting, and RNA interference demonstrated that the observed detrimental effects of caffeine on CSC were attributable specifically to the inhibition of the PIK kinase ataxia telangiectasia- and Rad3-related (ATR). Mechanistically, phosphorylation of CHK1 checkpoint homolog (*S. pombe*; CHK1) was significantly enhanced in CD133$^+$ as compared with CD133$^-$ cells on treatment with DNA interstrand-crosslinking (ICL) agents, indicating a preferential activation of the ATR/CHK1-dependent DNA-damage response in tumorigenic CD133$^+$ cells. Consistently, the chemoresistance of CD133$^+$ cells toward DNA ICL agents was overcome through inhibition of ATR/CHK1-signaling. In conclusion, our study illustrates a novel target to eliminate the tumorigenic CD133$^+$ cell population in colon cancer and provides another rationale for the development of specific ATR-inhibitors. STEM CELLS *2011;29:418–429*

Disclosure of potential conflicts of interest is found at the end of this article.

INTRODUCTION

According to the cancer stem cell (CSC) model, solid tumors may not be viewed as simple monoclonal expansions of functionally equal cancer cells. Instead, despite their clonal origin, only a fraction of tumor cells, termed CSC, "tumorigenic cells" or "tumor-initiating cells," appears to bear exclusive tumorigenicity based on functional assays of self-renewal and tumor initiation [1–3]. Increasing evidence suggests that among several other solid malignancies, the CSC model can also be applied to colon cancer. A CD133$^+$ subpopulation of colon cancer cells derived from primary lesions was shown to be highly enriched for tumorigenic colon CSC capable of

Author contributions: E.G.: conception and design, financial support, collection and assembly of data, data analysis and interpretation, manuscript writing, final approval of manuscript; P.C.H.: conception and design, collection and assembly of data, data analysis and interpretation, manuscript writing, final approval of manuscript; M.-T.M.: collection and assembly of data, data analysis and interpretation; J.G.M.: collection and assembly of data; A.Z.: collection and assembly of data; E.N.D.T.: data analysis and interpretation; A.P.: collection and assembly of data; C.E.: collection and assembly of data; J.W.E.: collection and assembly of data; J.R.: collection and assembly of data; B.R.-V.: provision of study material; M.H.: provision of study material; F.B.: conception and design, provision of study material; B.G.: conception, financial support; C.H.: conception and design, financial support, data analysis and interpretation, manuscript writing, final approval of manuscript. E.G. and P.C.H. contributed equally to this article.

Correspondence: Prof. Dr. Christopher Heeschen, M.D., Ph.D., Clinical Research Programme, Stem Cells & Cancer Group, Spanish National Cancer Research Centre (CNIO), Madrid, Spain. Telephone: +34 91 732 80 00; Fax: +34 91 224 69 31; e-mail: cheeschen@cnio.es Received July 19, 2010; accepted for publication December 22, 2010; first published online in STEM CELLS *EXPRESS* February 4, 2011. 1066-5099/2009/$30.00/0 doi: 10.1002/stem.595

self-renewal and recapitulation of the bulk tumor population [4, 5]. Based on the demonstrated principle of CSC as the root of the tumor and their resistance toward conventional chemotherapy [3, 6–8], the development of approaches aiming at the specific eradication of CSC in solid tumors represents an innovative goal for improved cancer treatment.

Recently, cell cycle modulation through checkpoint abrogation emerged as a promising approach in cancer therapy. In contrast to normal cells, cancer cells appear to be selectively sensitive toward treatment with inhibitors of checkpoint kinases, especially when these agents were combined with DNA interstrand-crosslinking (ICL) agents [9, 10]. Importantly, a preferential activation of the DNA-damage response (DDR), comprising both amplified DNA-damage checkpoint activation and increased repair of DNA-damage, has been described as likely mechanism of CSC drug- and irradiation-resistance in several tumor entities [11, 12]. However, the impact of checkpoint abrogation through inhibition of checkpoint kinases specifically on the CSC population in colon cancer has not yet been systematically explored. Therefore, we investigated the effects of checkpoint-modulation through inhibition of phosphoinositide 3-kinase-related (PIK) kinases specifically on the exclusively tumorigenic $CD133^+$ colon cancer cell population in multiple model systems using primary colon cancer cells and human colon cancer cell lines for a comprehensive mechanistic investigation.

Materials and Methods

Cell Lines, Primary Colon Cancer Samples, and Cell Culture

The human colon cancer cell lines DLD1, Colo320, and RKO were purchased from the American Type Culture Collection (ATCC, Wesel, Germany, www.atcc.org). COGA-12 was kindly provided by M. Ogris (Department of Pharmacy, Ludwig-Maximilian-University Munich, Germany). RKO cells harboring an inactivating deletion of *FANCC* and *FANCG*, respectively, and DLD1 cells harboring the Seckel mutation of the ataxia telangiectasia- and Rad3-related (*ATR*) gene have been described previously [13, 14]. Primary colon cancer cells for ex vivo experiments were established through subcutaneous xenografting in nude mice according to a protocol described earlier [15]. Importantly, all in vivo-expanded cell lines used in our study were transplanted as tissue, using their natural environment for expansion according to a previously established protocol [16] and analyzed during early passages: CCR004 (passage 5), CCR005 (passage 5), CCR010 (passage 2), CCR14 (passage 8–10), and CCR19 (passage 3). All cell lines were maintained in Dulbecco's modified Eagle's medium (DMEM) medium supplemented with 10% fetal calf serum and penicillin-streptomycin (1%) and incubated at 37°C and 5% CO_2. Cells were treated with caffeine (Sigma-Aldrich, Munich, Germany, www.sigmaaldrich.com), UCN-01 (Sigma), SB-218078 (Merck KG, Darmstadt, Germany, www.merck.de), RAD001 (Novartis GmbH, Nuremberg, Germany, www.novartis.de), KU-55399 (Sigma), cisplatin (cis-diammineplatinum(II)-dichloride; Sigma).

Sphere Formation Assays

CSC spheres were cultured in DMEM-F12 (Invitrogen, Karlsruhe, Germany, www.invitrogen.com) supplemented with B-27 (Invitrogen) and basic fibroblast growth factor (bFGF) (PeproTech EC, London, U.K., www.peprotech.de). A total of 10,000 cells per milliliter were seeded in ultra-low attachment plates (Corning B.V., Schiphol-Rijk, The Netherlands, www.corning.com) to avoid cell adhesion and subsequent differentiation. Three to five days after treatment, four visual fields of at least two wells were counted. Three or more independent experiments were performed for each group. When no sphere formation occurred, the remaining single cells were kept under sphere culture conditions for up to 12 days to ensure a sufficient observation time. For primary cancer cell experiments, in vivo-expanded primary colon cancer samples from five different patients were digested with collagenase (Stem Cell Technologies, Vancouver, Canada, www.stemcell.com) for 20 minutes at 37°C. Dead cells were removed using a kit according to the manufacturer's instructions (Miltenyi, Bergisch-Gladbach, Germany, www.miltenyibiotec.com). Sphere formation capacity was assessed 3–11 days after treatment. For sphere reformation, single-cell suspensions were plated in normal sphere medium after 11 days of treatment. Spheres were defined as morphologically characteristic three-dimensional structures of approximately >35 μm, containing an average of 50 cells. According to this definition, all sphere formation experiments were evaluated by two-blinded observers (P.C.H./C.H. or M.T.M./C.H., respectively).

Animals and Transplantation of Human Colon Cancer Cells

Female Naval Medical Research Institute nude mice (NMRI-nu/nu, Janvier, Le Genest-Saint-Isle, France, www. janvier-europe.com) at 8–12 weeks were used. All animal protocols were approved by the Institutional Animal Care and Use Committee of the CNIO or by the Administrative Panel on Laboratory Animal Care (Government of Upper Bavaria, Germany). Colon cancer cells were injected under the renal capsule of anesthetized mice as described previously [4]. One day prior to cell transplantation, mice were sublethally irradiated (350 cGy). Then, single-cell suspensions were suspended in a 1:1 mixture of media and Matrigel (BD Biosciences, Heidelberg, Germany, www.bdbiosciences.com) and 5×10^5 cancer cells were injected using a PB600 repeating dispenser (Hamilton AG, Bonaduz, Switzerland, www.hamilton-ag.ch). Tumorigenicity of DLD1 $ATR^{+/+}$ cells was validated in two independent experiments ($n = 10$ mice, 100% take rate) and served as a control for all animal experiments involving DLD1 cells. Additionally, all experiments were microscopically evaluated to confirm sufficient cell grafting (through confirmation of single tumor cells or small aggregates, respectively, under the renal capsule) and to exclude macroscopically invisible small tumor formation in macroscopically tumor-negative animals. For s.c. transplantation models, single-cell suspensions containing 2×10^4 xenograft-derived primary cells were suspended as described above and implanted s.c. into both flanks of nude mice.

Flow Cytometry

For the identification and FACSorting of colon CSC, cells were stained with allophycocyanin- or phycoerythrin-labeled CD133/1 (Miltenyi) or epithelial cell adhesion molecule (EpCAM) (BD) antibodies or appropriate isotype-matched control antibodies. Dead cells were excluded using 7-amino-actinomycin D (7-AAD) (BD Biosciences) or 4',6-diamidino-2-phenylindole (Sigma). Cell cycle analysis was performed using a 5-bromo-2-deoxyuridine (BrdU) flow cytometry kit (BD) according to the manufacturer's instructions. For detection of apoptotic cells, costaining with 7AAD and Annexin V-fluorescein isothiocyanate (FITC) (BD) was performed. Caspase inhibitors Z-VAD-FMK (R&D Systems, Minneapolis, MN, www.rndsystems.com), Z-IETD-FMK (BD), and Z-LEHD-FMK (BD) were applied at 20 μM for 3 hours, followed by caffeine treatment. Flow cytometry was performed on a FACSCanto II, FACSorting on a FACSAria II

(both BD), and data were analyzed using FlowJo 9.0.2 (Ashland, OR, www.flowjo.com).

siRNA-Mediated ATR Protein-Depletion

DLD1 cells at 30%–50% confluence were transfected using oligofectamine (Invitrogen) and siRNA directed against either ATR (Hs ATR 12 HP, Qiagen, Hilden, Germany, www.qiagen.com) or CHK1 checkpoint homolog (*S. pompe*) (CHK1) (Hs CHEK1 7, HP, Qiagen) or non-coding sequences of the β-galactosidase (β-gal) gene (sense, UUAUGCCGAUC GCGUCACAUU; antisense, UGUGACGCGAUCGGCAUA AUU; Fisher, Schwerte, Germany, www.de.fishersci.com). siRNAs were used at final concentrations of 5 nM (ATR siRNA) or 50 nM (CHK1 and β-gal siRNA). After transfection for 4 hours, serum-containing medium was added. To ensure efficient long-term downregulation, siRNAs were applied repetitively (according to a previously established protocol at 48, 96, 168, 216, 264, 336, and 384 hours for ATR and at 48, 96, 168, and 216 hours for CHK1). Efficiency of ATR and CHK1 protein-depletion was evaluated using Western blotting.

Western Blotting

Western blotting was performed using standard protocols. Briefly, equal amounts of protein were separated by SDS-polyacrylamide gel electrophoresis and transferred to polyvinylidene fluoride membranes. After blocking, the membranes were incubated overnight with the primary antibody either against ATR (Santa Cruz Biotechnology, Santa Cruz, CA, www.scbt.com), pChk1 (Cell Signaling, Danvers, MA, www.cellsignal.com), β-actin or glyceraldehyde 3-phosphate dehydrogenase (Sigma), washed three times, and probed with the corresponding secondary antibodies (1:10,000; Santa Cruz) for 2 hours. Enhanced chemiluminescence detection was performed according to the manufacturer's instructions (Little Chalfont, U.K., www.gelifesciences.com).

Immunohistochemistry

For histological evaluation, tumor tissue was fixed in formalin and embedded in paraffin. Histological staining for cytokeratin 5, 6, 8, 17, 19 (Dako, Hamburg, Germany, www.dako.com), and hemalaun (Sigma) confirmed the nature of the tumors. For immunostaining, slides were incubated for 1 hour with a Ki67 antibody (Abcam, Cambridge, U.K., www.abcam.com) followed by a biotin-labeled secondary antibody (Cytomed, Baden-Baden, Germany, www.cytomed.de) and streptavidin-FITC for detection. CSC were identified by Texas Red-labeled antibodies for CD133 (Abcam). Cell nuclei were counterstained with Sytox Blue (Invitrogen). Sections were analyzed with a Leica SP5 confocal microscope.

Statistical Analyses

Results for continuous variables are presented as means $\pm$ SEM. Treatment groups were compared with the independent sample's t test. Pairwise multiple comparisons were performed with the one-way analysis of variance (two-sided) with Bonferroni adjustment. p values $<.05$ were considered statistically significant. All analyses were performed using SPSS 17.0 (SPSS Inc., Chicago, IL, www.spss.com).

Results

Tumorigenicity Is Restricted to the CD133$^+$ Cell Fraction in DLD1 Colon Cancer Cells

We first evaluated whether CD133 represents a suitable marker for the identification of tumor-initiating cells in the colon cancer cell line DLD1 as a versatile model system. Consistent with previous findings for primary human colon cancer cells [4, 5], we detected a small fraction of CD133$^+$ cells in DLD1 cells (Fig. 1A). Separation of DLD1 subsets on the basis of CD133 expression resulted in the significant enrichment of CD133$^+$ cells and the efficient negative selection of CD133$^-$ cells (Fig. 1B, second and third panel). CD133$^-$ cells, subsequently kept under adherent culture conditions for 14 days, were not capable of producing CD133$^+$ cells, whereas CD133$^+$ cells readily generated a heterogeneous population of CD133$^+$ and CD133$^-$ cells compositionally comparable with that of unsorted cells (Fig. 1B, first and fourth panel). Sphere formation capacity as a surrogate for CSC activity and in vitro tumorigenicity [5, 7] was significantly lower for CD133$^-$ cells as compared with CD133$^+$ cells (Fig. 1C). The depletion of the tumor-initiating fraction in a cancer cell population is expected to decrease the in vivo tumorigenicity of the remaining cells. Therefore, we assessed the ability of sorted CD133$^+$ and CD133$^-$ DLD1 cells to engraft and give rise to tumors when implanted under the renal capsule of sublethally irradiated athymic nude mice [4]. Although 10^4 CD133$^-$ cells did not form tumors in any of the mice, the injection of 10^4 CD133$^+$ cells resulted in macroscopic tumor lesions in all animals within 30 days (Fig. 1D). Therefore, CD133 can serve as a suitable marker for the identification of the tumorigenic cell fraction in DLD1.

Depletion of the CD133$^+$ Cell Fraction By Caffeine Treatment Abrogates In Vitro and In Vivo Tumorigenicity of Colon Cancer Cells

Treatment with caffeine, an unspecific inhibitor of checkpoint-modulating PIK kinases, at 0.2–5 mM over a time period of 21 days every 2 days dose-dependently depleted the CD133$^+$ cell fraction of DLD1 cells (Fig. 2A). This effect became statistically significant at 5 mM (Fig. 2B). Caffeine treatment of another colon cancer cell line, COGA12, had a similar effect, ruling out cell line-specific artifacts (Fig. 2C).

As sphere formation capacity serves as a surrogate marker for CSC activity and in vitro tumorigenicity of cancer cells in solid tumors [5, 8], DLD1 cells were next treated over a time period of 21 days every 2 days with caffeine at 5 mM and consecutively, sphere formation was evaluated. Although untreated control cells readily formed spheres within 3–5 days, caffeine-treated cell populations exhibited a strongly diminished sphere formation capacity (Fig. 2D).

As the depletion of the tumor-initiating CD133$^+$ cell fraction is expected to decrease the in vivo tumorigenicity of the remaining subpopulation, DLD1 cells were next treated over a time period of 21 days every 2 days with caffeine at 1 and 5 mM and then implanted under the renal capsule of nude mice. Thirty days after cell implantation, tumor take rate and tumor size were assessed (see Fig. 2E for experimental setup). We observed a dose-dependent decrease of the in vivo tumorigenicity of the cell populations pretreated with caffeine as shown by a decreased to completely absent tumor take rate (Fig. 2F). In contrast, large tumor formation was observed in all animals of the control group (Fig. 2G).

Depletion of the CD133$^+$ Cell Fraction by Caffeine Treatment Abrogates In Vitro and In Vivo Tumorigenicity of Primary Colon Cancer Cells

To generalize our findings beyond the setting of established cell lines, we expanded primary colon cancer cells from surgical tumor specimens using an in vivo xenograft model modified from Jimeno et al. [15]. Xenograft-derived tumor

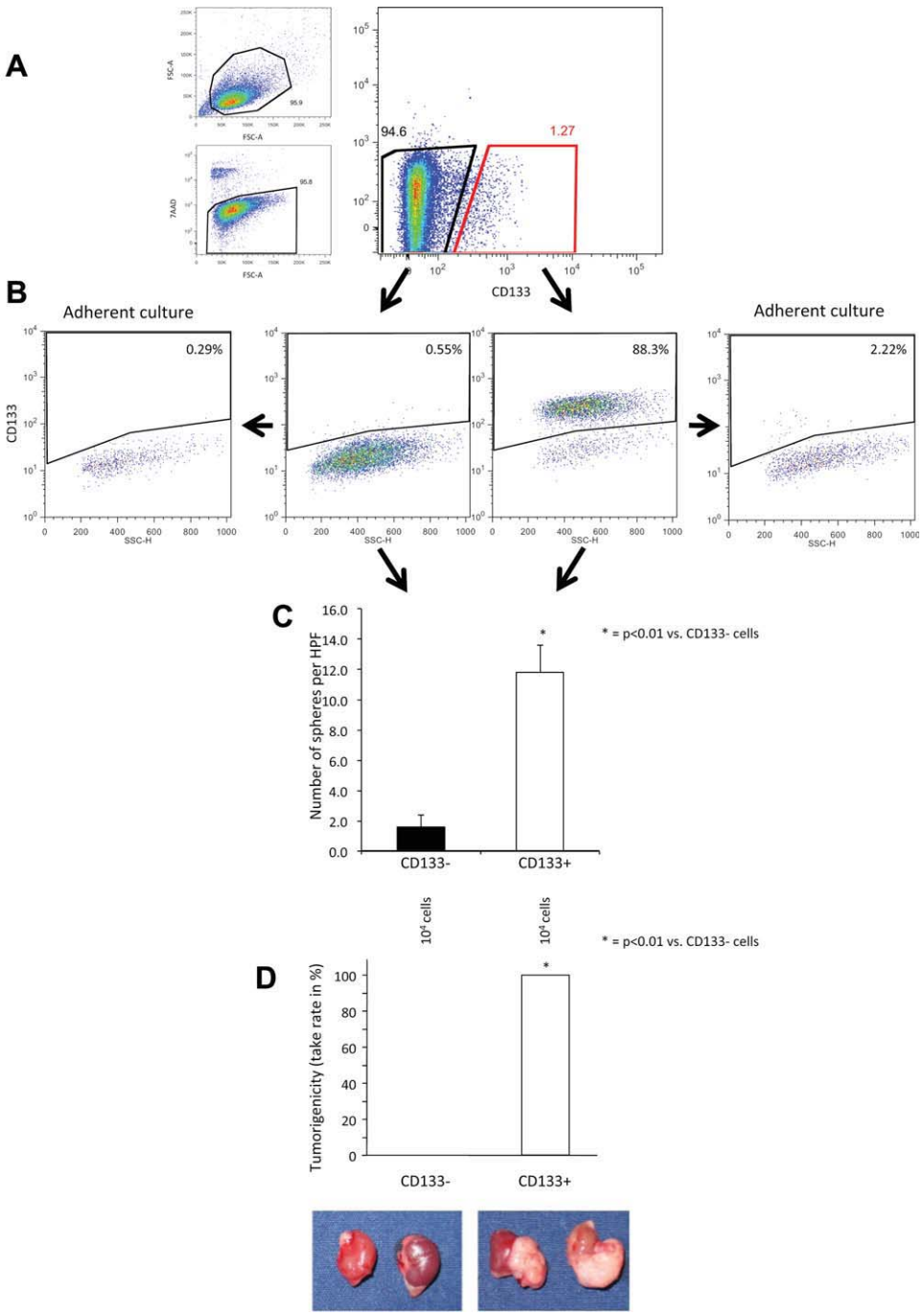

Figure 1. $CD133^+$ as a marker for the tumorigenic fraction of DLD1 colon cancer cells. CD133 expression in DLD1 colon cancer cells **(A)** before and **(B)** after FACS according to CD133 expression (second panel $CD133^-$ cells, third panel $CD133^+$ cells). Subsequent adherence culture of sorted $CD133^+$ (fourth panel) and $CD133^-$ cells (first panel). **(C):** Sphere formation capacity of $CD133^-$ and $CD133^+$ cells. **(D):** Tumor take rate after injection of 10^4 $CD133^+$ or $CD133^-$ cells, respectively, under the renal capsule of nude mice ($n = 5$ per group): Statistical evaluation (upper panel) and representative macroscopic images (lower panel). Note that the connective tissue adhering to the kidneys on the left picture represents adipose tissue. Abbreviations: 7AAD, 7-aminoactinomycin D; FSC-A, forward scatter - area; SSC-H, side scatter - height.

specimens of five patients were dissociated and single-cell suspensions investigated for surface expression of CD133 prior to and 11 days after caffeine treatment. Coexpression of EpCAM was used to discriminate tumor cells from potential contaminating endothelial or hematopoietic stem and progenitor cells. We found a significant decrease of the $EpCAM^+$ $CD133^+$ cell fraction in primary tumor cells after caffeine treatment (Fig. 3A, left panel). Importantly, we observed single viable cells, which were not clonally expanding under these conditions by the end of the treatment period (Fig. 3A, right panel), although apparently lower in numbers as compared with control cells, thus confirming a preferential targeting of the clonally expanding cells. Consistently, caffeine-treated primary colon cancer cells, although viable, demonstrated a strongly diminished sphere formation capacity as compared with control cells (Fig. 3B).

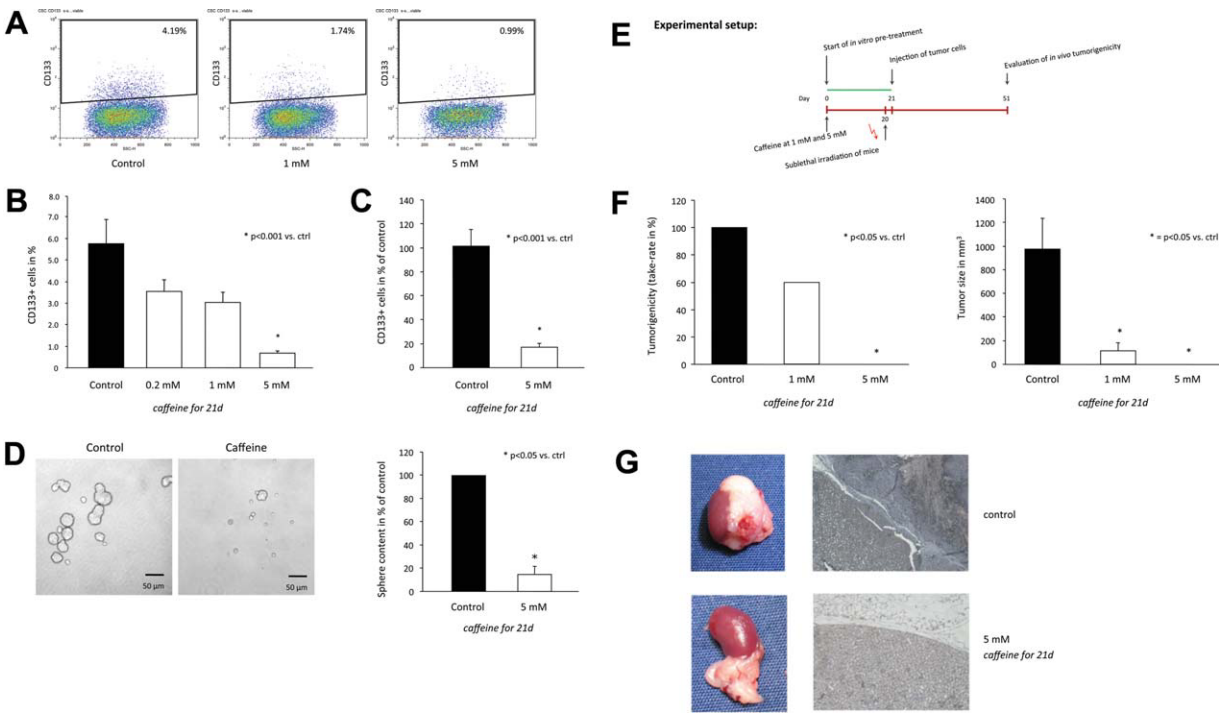

Figure 2. Dose-dependent depletion of CD133$^+$ cells after caffeine treatment and reduced in vitro and in vivo tumorigenicity of the remaining cell population: CD133$^+$ fraction of DLD1 cells treated with caffeine at the indicated concentrations for 21 days. **(A):** Representative results and **(B)** statistical evaluation ($n = 5$). **(C):** CD133$^+$ fraction of COGA12 cells treated with caffeine for 21 days ($n = 3$). **(D):** Representative images (left two panels) and statistical evaluation ($n = 3$; right panel) of sphere formation capacity of DLD1 cells treated with caffeine or control for 21 days. **(E):** Experimental setup for the in vivo experiments. **(F):** In vivo tumorigenicity, evaluated 30 days after injection of DLD1 cells under the renal capsule of nude mice: tumor take rate (left panel) and volume (right panel) after implantation of cells treated with control ($n = 10$) or caffeine at 1 mM ($n = 5$) or 5 mM ($n = 7$), respectively. **(G):** Representative macroscopic and microscopic pictures of tumor formation after injection of untreated control cells (upper panel) or cells treated with caffeine for 21 days (lower panel). Abbreviations: CSC, cancer stem cell; SSC-H, side scatter - height.

As we detected a small proportion of viable CD133$^+$ cells after caffeine treatment, representing either CD133$^+$ nontumorigenic cells or surviving tumorigenic cells, we performed sphere reformation assays after caffeine treatment. Although control cells reproducibly generated second generation spheres, no sphere formation was observed in the caffeine-pretreated cells, when cultured in caffeine-free medium (Fig. 3C). Finally, dissociated control or caffeine pretreated single-cell suspensions, derived from xenograft-derived tumor specimens from three patients, were implanted s.c. in the respective flanks of the same mice to allow direct comparisons and to exclude interindividual take rate variability. During an observation period of 100 days, we observed a reduced tumor take rate, a decreased average size of engrafted tumors, and a significantly higher event-free long-term survival in the caffeine-treated group (Fig. 3D).

Caffeine Treatment Increases Proliferation and Apoptosis of CD133$^+$ Colon Cancer Cells

To elucidate the mechanism underlying the caffeine-mediated depletion of the tumorigenic CD133$^+$ cell fraction, we compared the effects of caffeine on proliferation of and apoptosis in CD133$^+$ cells versus CD133$^-$ cells. For technical reasons, we used colon cancer cell lines as a model system for these experiments. DLD1 cells were treated over a time period of up to 7 days with caffeine at 5 mM. Consecutively, BrdU or Annexin V staining along with concomitant CD133 staining was performed to separately analyze CD133$^+$ and CD133$^-$ cells with regard to proliferation and apoptosis. In the control group, 10% of CD133$^-$ cells and 17% of CD133$^+$ cells showed an early BrdU incorporation by 2 hours, while up to 96% of CD133$^-$ cells, but only 56% of CD133$^+$ cells had incorporated BrdU by 96 hours, indicative of a quiescent subset in the CD133$^+$ fraction. Caffeine treatment caused an earlier increase of BrdU-incorporating cells in both the CD133$^-$ and the CD133$^+$ fraction. Of note, the amount of BrdU-incorporating CD133$^+$ cells increased to 87% at 96 hours, suggesting a caffeine-induced activation of a formerly quiescent CD133$^+$ subset (Fig. 4A, 4B).

In a time-lapse analysis using AnnexinV as marker of early apoptosis, we observed an initial rapid decline of CD133$^+$ cell content after caffeine treatment, followed by a subsequent slower decline (Fig. 4C). Consistently, the fraction of CD133$^+$ AnnexinV$^+$ cells was rather high (up to 8%) during the initial 72 hours, although a smaller yet sustained fraction of CD133$^+$ AnnexinV$^+$ cells was observed up to 168 hours, presumably representing the quiescent CSC fraction progressively recruited to enter an active cell cycle. As apoptosis can be initiated via either the intrinsic (involving activation of caspase 9) or the extrinsic pathway (cleavage of caspase 8) [17], DLD1 cells were next preincubated using either pancaspase-, caspase 8-, or caspase 9-inhibitors before caffeine treatment. Incubation with the pan-caspase inhibitor strongly decreased the fraction of CD133$^+$ AnnexinV$^+$ cells after subsequent caffeine treatment. However, inhibition of either caspase 8 or caspase 9 alone was also sufficient to decrease apoptosis (Fig. 4D), suggesting that caffeine initiated apoptosis through cleavage of caspase 8, but that the recruitment of caspase 9 by a mitochondrial amplification loop was

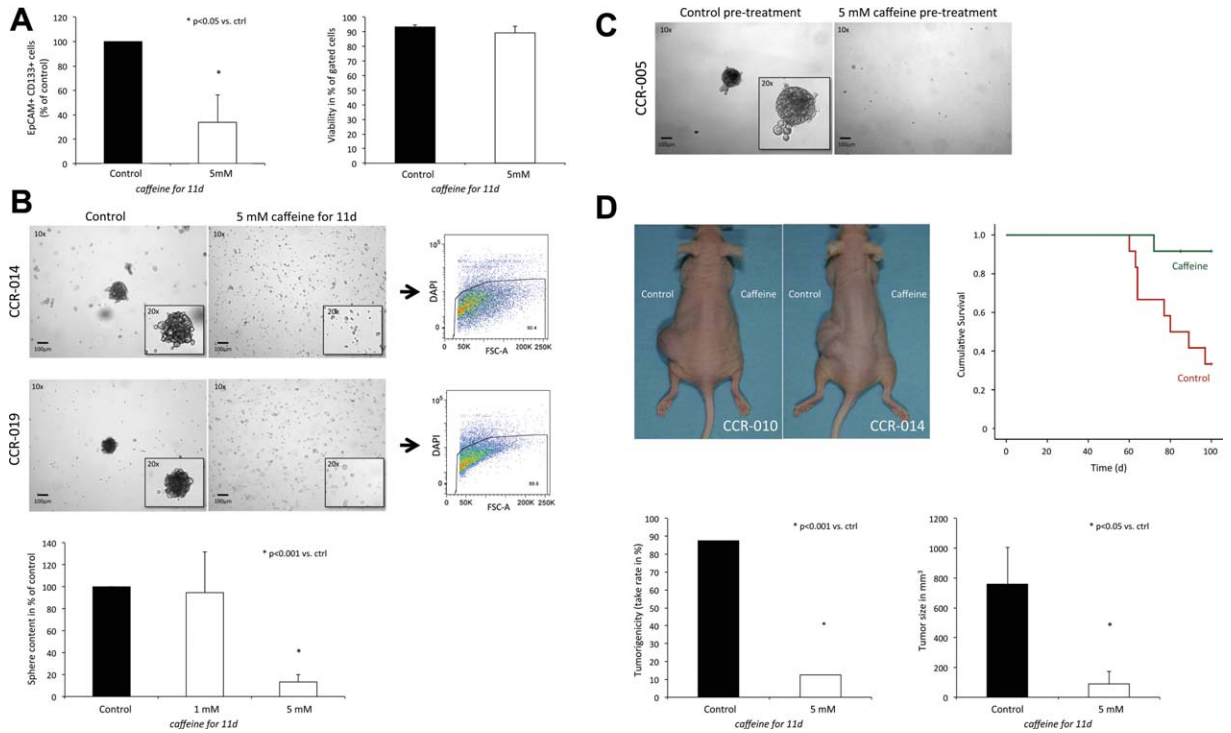

Figure 3. Effects of caffeine on the CD133$^+$ fraction of xenograft-derived primary colon cancer cells. Dissociated single cancer cells, derived from xenograft-expanded surgical colon cancer specimens from five patients, treated for 11 days with either control or caffeine at the indicated concentrations. **(A):** Quantification of the EpCAM$^+$ CD133$^+$ cell fraction (left panel) and viability of the gated cells (right panel; $n = 4$). **(B):** Representative pictures of sphere formation assays (upper left four panels) and assessment of cell viability after caffeine treatment (upper right two panels) for CCR-014 and CCR-019 primary tumor cells. Statistical evaluation is provided for all five tumors ($n = 3$ experiments for 1 mM caffeine, $n = 10$ experiments for 5 mM caffeine; lower panel). **(C):** Caffeine pretreated primary cells, seeded into medium without caffeine. Representative pictures of sphere reformation after 9 days. **(D):** Caffeine- or control-treated primary tumor cells, implanted s.c. into nude mice ($n = 7$ for CCR-010, $n = 5$ for CCR-014, $n = 4$ for CCR-005). Representative pictures of tumor-bearing mice (upper left two panels); Kaplan-Meier curve depicting cumulative event-free long-term survival (event = tumor growth exceeding 1 cm^3; upper right panel). Statistical evaluation is provided for tumorigenicity (lower left panel) and tumor size (lower right panel). Abbreviations: DAPI, 4',6-diamidino-2-phenylindole; EpCAM, epithelial cell adhesion molecule; FSC-A, forward scatter - area.

additionally required for the activation of effector caspases in the CSC fraction.

Caffeine-Induced Depletion of CD133$^+$ Colon Cancer Cells Is Mediated by ATR

Caffeine acts as an unspecific inhibitor of the checkpoint-modulating PIK kinases ataxia telangiectasia mutated (ATM), ATR, and mammalian target of rapamycin (MTOR), without being a global inhibitor of protein kinase activities [18]. To identify the signaling cascade mediating the caffeine-induced depletion of tumorigenic CD133$^+$ cells, we used KU-55399 for ATM inhibition [19] and RAD001 for MTOR inhibition [20]. Because of the lack of ATR-inhibitors and as CHK1 represents the major effector kinase of ATR, we additionally applied the potent, but in comparison with the highly specific ATM inhibitors, less-specific CHK1 inhibitor UCN-01 and its analog SB218078 [21–25]. UCN-01 was chosen as it currently represents the most clinically advanced CHK1 inhibitor, which has already undergone clinical trials, whereas SB218078 was chosen due to its better specificity as it exerts much less inhibitory activity against protein kinase C as compared with UCN-01 [26]. Although treatment with either RAD001 or KU-55399 had no significant effects, UCN-01 and SB218078 both caused a significant decrease of CD133$^+$ cells, suggesting that inhibition of either CHK1 or the upstream PIK kinase ATR mediated the caffeine-induced effects (Fig. 4E).

DLD1 Cells Harboring an Inactivating ATR Mutation Lack the Tumorigenic CD133$^+$ Cell Fraction

To further support that disruption of ATR function was responsible for the caffeine-induced effects, we applied a genetic knock-in model. The hypomorphic *ATR* splice-site "Seckel" mutation $2101^{A\rightarrow G}$ leads to a subtotal depletion of ATR protein but has no gross effects on cancer cell growth or viability [14, 27]. Therefore, parental DLD1 ($ATR^{+/+}$) cells, constitutively expressing ATR protein, were compared with cells homozygously harboring the Seckel mutation ($ATR^{s/s}$ cells) [14], which express no detectable ATR protein (Fig. 5A). $ATR^{+/+}$ and $ATR^{s/s}$ cells were long-term passaged for at least 3 months before analysis of CD133 expression status. Although $ATR^{+/+}$ cells displayed a CD133$^+$ cell population ranging from 3% to 8% (Fig. 5B) when assessed at different time points during cell culture, $ATR^{s/s}$ cells exhibited a near absent CD133$^+$ cell fraction. Consistently, $ATR^{s/s}$ cells were severely impaired in sphere formation capability (Fig. 5C) and completely unable to form tumors in nude mice (take rate 0%; $n = 10$; Fig. 5D, 5E).

Depletion of the Tumorigenic CD133$^+$ Cell Fraction on Continuous siRNA-Mediated ATR-Knockdown

To exclude potential artifacts that might occur due to clonal variability in the *ATR* knock-in experiments, we additionally assessed the effects of continuous ATR protein-depletion on

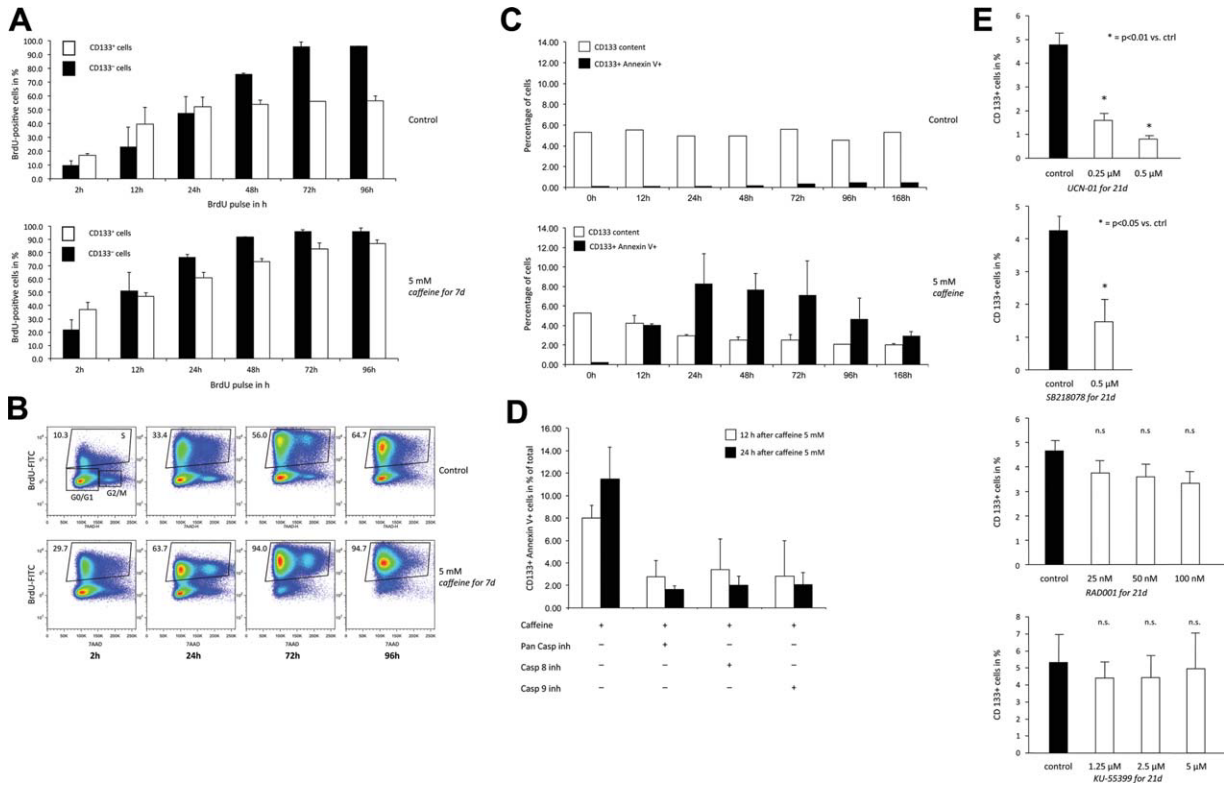

Figure 4. Mechanism of the caffeine-induced depletion of the CD133$^+$ cell fraction. **(A):** BrdU-incorporating fraction of CD133$^+$ DLD1 cells after treatment for 7 days with control (upper panel) or caffeine (lower panel) at 2–96 hours after treatment. **(B):** Representative flow cytometric assessments of cell cycle profiles of CD133$^+$ DLD1 cells after treatment for 7 days with control or caffeine at 2–96 hours after treatment. **(C):** CD133$^+$ fraction and CD133$^+$ Annexin V$^+$ subset of DLD1 cells, either treated with control (upper panel) or caffeine (lower panel), assessed at the indicated time points. **(D):** CD133$^+$ Annexin V$^+$ fraction of caffeine-treated DLD1 cells pretreated with the indicated caspase inhibitors for 2 hours. **(E):** Statistical evaluation ($n = 3$) of the CD133$^+$ fraction of DLD1 cells treated with the indicated PIK kinase or checkpoint inhibitors, respectively, at the indicated concentrations for 21 days. Abbreviations: 7AAD, 7-aminoactinomycin D; BrdU, 5-bromo-2-deoxyuridine; FITC, fluorescein isothiocyanate.

unselected cancer cells, using repetitive applications of ATR-siRNA over a time period of 384 hours. ATR protein-depletion efficiency of >80% was confirmed for all time points starting from 96 hours up to 384 hours (Fig. 6A). ATR siRNA-treated cells displayed a time-dependent reduction of the CD133$^+$ cell fraction when compared with mock-transfected or control siRNA-transfected cells, starting at 96 hours after transfection (Fig. 6B). After 384 hours of repetitive ATR-siRNA treatment, the cells were implanted under the renal capsule of nude mice, and tumor take rate was assessed 30 days later (Fig. 6C). The ATR siRNA-treated cells displayed a reduced but not completely absent capability to form tumors (take rate 33%; $n = 6$) as compared with control cells (Fig. 6D). Two mice bore clearly diminutive tumors, approximating 2 mm^3 in both cases, as compared with 970 mm^3 on average observed in control mice. In these diminutive tumors, we detected only sparse proliferation activity and rare presence of CD133$^+$ cells (<1 cell per high-power field for ATR-siRNA-treated cells vs. 6.1 ± 2.7 for control cells; Fig. 6E).

No Significant Depletion of the Tumorigenic CD133$^+$ Cell Fraction on Continuous siRNA-Mediated CHK1-Knockdown

Analogous to the above experiments using ATR siRNA, a similar set of experiments was performed for ATR's major effector kinase CHK1, using repetitive applications of CHK1 siRNA. In contrast to ATR siRNA-treated cells, which displayed a strong reduction of the CD133$^+$ cell fraction as soon as 96 hours after transfection, CHK1 siRNA-treated cells, even though efficiently depleted of CHK1 protein, did not display a significant reduction of the CD133$^+$ cell fraction over a time period of 264 hours when compared with control cells (data not shown).

Depletion of CD133$^+$ Colon Cancer Cells on ATR-Inhibition Is Fanconi Anemia Pathway-Independent

As ATR-inhibition causes disruption of the Fanconi anemia (FA) DNA-repair pathway [28], we tested whether this pathway contributed to the ATR inhibition-mediated effects on CD133$^+$ cells. The CD133$^+$ cell fraction of RKO colon cancer cells was compared with the CD133$^+$ fraction of RKO cells engineered to harbor inactivating deletions of either the *FANCC* or *FANCG* gene [13]. No significant differences were observed in this FA model, excluding the FA pathway as a major contributing factor to the ATR inhibition-induced depletion of CD133$^+$ cells (data not shown).

Induction of Stalled Replication Forks Increases the Effects of ATR/CHK1-Inhibition on the CD133$^+$ Cell Fraction

ATR acts as a central regulator of the replication checkpoint and participates in the detection and repair of endogenous and exogenously induced stalled replication forks (SRF) via

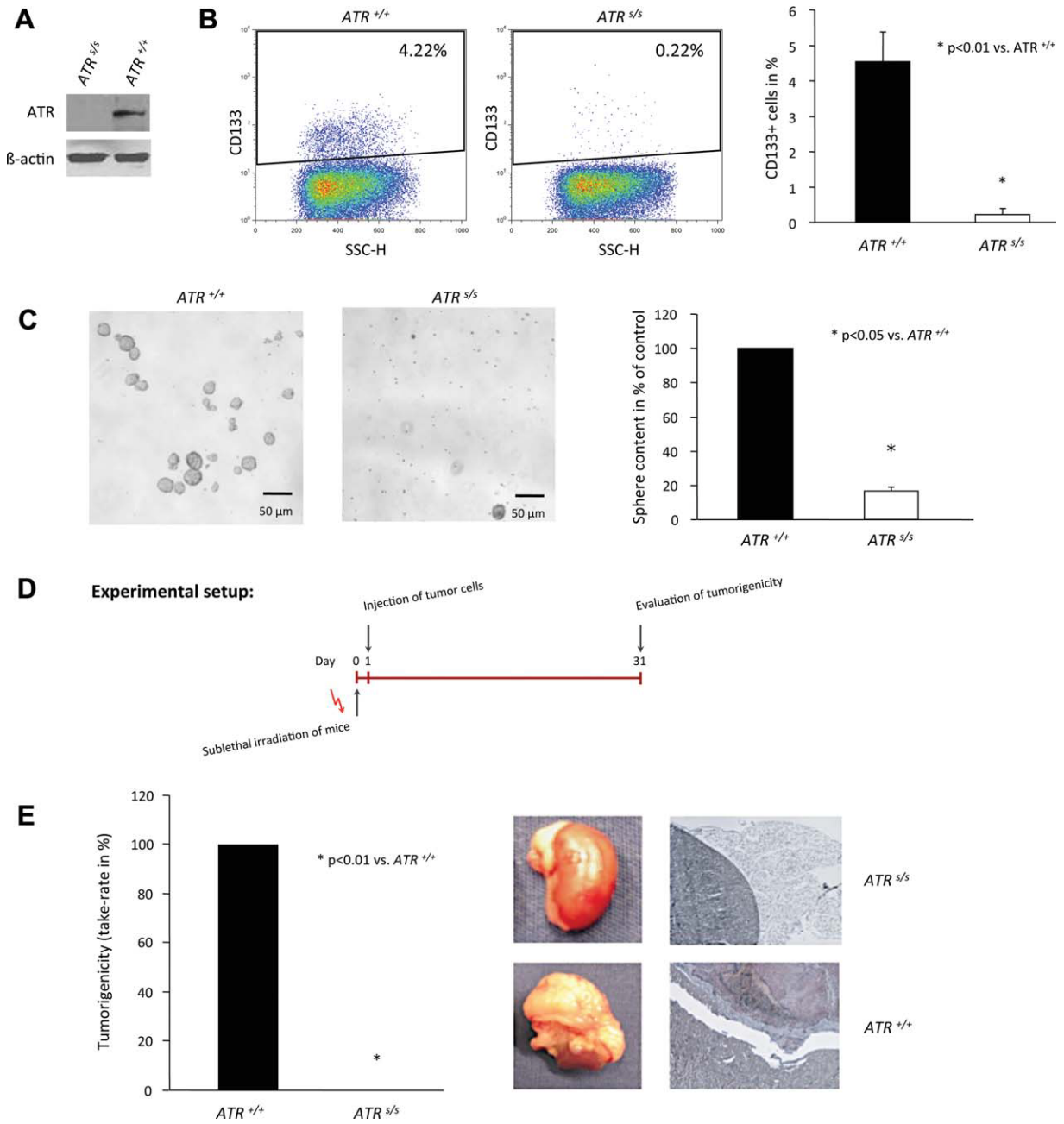

Figure 5. Reduced tumorigenicity of colon cancer cells harboring an inactivating *ATR* mutation. **(A):** ATR protein content of $ATR^{+/+}$ and $ATR^{s/s}$ cells, as assessed by Western blotting. **(B):** $CD133^{+}$ cell fraction of $ATR^{+/+}$ and $ATR^{s/s}$ cells: representative results (left two panels) and statistical analysis ($n = 5$, assessed at five time points during culture, right panel). **(C):** Sphere formation capacity of $ATR^{+/+}$ cells and $ATR^{s/s}$ cells: representative results (left two panels) and statistical evaluation ($n = 3$, right panel). **(D):** Experimental setup for the in vivo experiments. **(E):** In vivo tumorigenicity, evaluated 30 days after injection of $ATR^{+/+}$ ($n = 10$) or $ATR^{s/s}$ ($n = 10$) cells under the renal capsule of nude mice: statistical evaluation (left panel) and representative macroscopic and microscopic pictures (right panel). Abbreviations: ATR, ataxia telangiectasia and Rad3 related; SSC-H, side scatter - height.

phosphorylation of the checkpoint kinase CHK1 [29]. Consistent with previous reports describing amplified checkpoint activation in some CSC [11, 12], upregulation of CHK1 phosphorylation was significantly more pronounced in the $CD133^{+}$ than in the $CD133^{-}$ cell fraction on treatment with the SRF-inducing ICL-agent mitomycin C, when compared with the respective untreated cell fractions. Importantly, the increased CHK1 phosphorylation levels in the $CD133^{+}$ cell fraction were not merely ascribable to increased levels of total CHK1 protein (Fig. 7A, left panel). As ICL-inducing platinum compounds are more commonly used than mitomycin C for the treatment of colorectal cancer in the clinical setting, the above results were additionally validated using cisplatin, a classic platinum ICL-agent, yielding similar results (Fig. 7A, right panel).

To test whether consequently, ICL-agents would synergistically add to the preferential depletion of $CD133^{+}$ cells through inhibition of the ATR/CHK1 axis, DLD1 cells were treated with caffeine, the CHK1-inhibitor SB218078 or the ICL-agent cisplatin alone, or using different combinations of

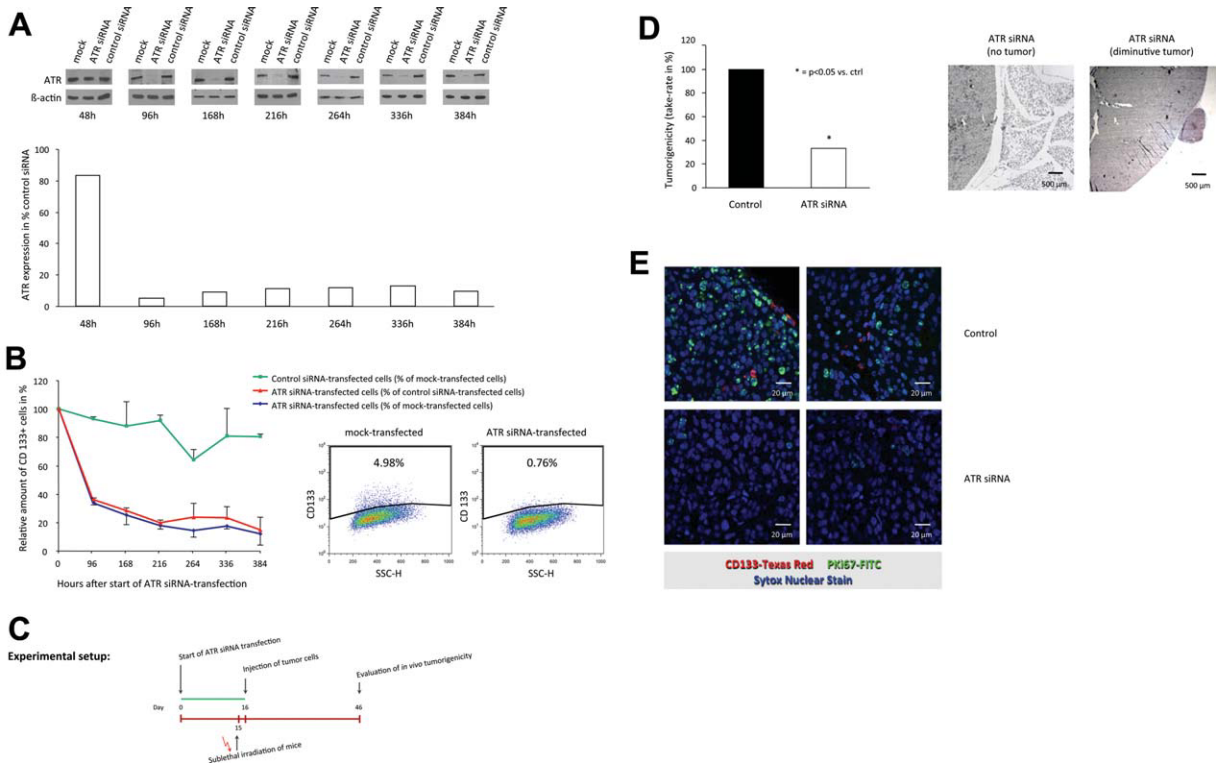

Figure 6. Decreased CD133$^+$ fraction and reduced tumorigenicity of colon cancer cells on ATR protein-depletion: **(A):** Representative results from one of two experiments, showing ATR protein content of mock-, ATR siRNA-, and control siRNA-transfected DLD1 cells at the indicated time points, as assessed by Western blotting (upper panel), and corresponding densitometric quantification (lower panel). **(B):** Flow cytometric assessment of the relative CD133$^+$ content of mock-, ATR siRNA-, and control siRNA-transfected DLD1 cells, compared with each other at the indicated time points (left panel). CD133$^+$ fraction of mock- or ATR siRNA-transfected cells after 384 hours of repetitive siRNA application (right two panels). **(C):** Experimental setup for the in vivo experiments. **(D):** In vivo tumorigenicity, evaluated 30 days after injection of ATR siRNA-transfected cells: statistical evaluation ($n = 6$, left panel) and representative microscopic pictures showing no or diminutive tumor growth, respectively (right two panels). **(E):** Histological analysis for the presence of CD133$^+$cells (red) in tumors from control- or ATR siRNA-transfected cells. Cell proliferation was assessed by Ki67 staining (green). Nuclei were identified by Sytox Blue staining (blue). Abbreviations: ATR, ataxia telangiectasia and Rad3 related; FITC, fluorescein isothiocyanate; SSC-H, side scatter - height.

these agents. Caffeine caused a significant decrease of CD133$^+$ cells as early as 5 days after initiation of treatment and a nearly complete elimination on longer treatment (21 days). Treatment with the CHK1-inhibitor SB218078 at 10 or 20 nM resulted in a significant decrease of CD133$^+$ cells only after 21 days (Fig. 7B). Consistent results were obtained when using Colo320 cells (Fig. 7C, left panel) and further supported by the observation that the CD133$^+$ AnnexinV$^+$ cell fraction inversely correlated with the total CD133$^+$ cell fraction (Fig. 7C, right panel). In contrast, we observed no decrease of CD133$^+$ cells on treatment with cisplatin alone at 6.6 μM for 2 days (Fig. 7D) in either DLD1 or Colo320, whereas pretreatment with either caffeine or SB218078 followed by treatment with cisplatin strongly reduced the CD133$^+$ fraction of both cell lines already after short-term treatment (Fig. 7E).

Discussion

We demonstrate here that inhibition of ATR function depletes the tumorigenic CD133$^+$ fraction of established colon cancer cell lines as well as xenograft-derived primary colon cancer cells. This effect translated into a markedly reduced tumorigenicity of the remaining cells, as shown by an impaired sphere formation capacity in vitro [5, 7] as well as a strongly reduced capability to form tumors in vivo. Consistent with previous reports describing amplified checkpoint activation and increased DNA repair to be distinct features of some CSC [11, 12], CD133$^+$ cells displayed a stronger activation of the ATR-dependent DDR on treatment with ICL-agents than did CD133$^-$ cells, as evidenced by a more pronounced increase in phosphorylation of ATR's major effector kinase CHK1. Importantly, the depletion of CD133$^+$ cells was enhanced on subsequent treatment with ICL-agents, suggesting that inhibition of ATR might reverse the chemoresistance of CSC toward ICL-agents in the clinical setting and could thus serve as a novel therapeutic strategy for patients suffering from colon cancer.

As the PIK kinases ATM, ATR, MTOR, and DNA-PK all play pivotal roles in cell cycle checkpoint functions and all except DNA-PK are effectively inhibited by caffeine [18], caffeine was used as a screening approach to modulate checkpoint function in colon cancer cells. Caffeine treatment virtually abolished the CD133$^+$ cell fraction and was accompanied by a decreased in vitro and in vivo tumorigenicity of the remaining cell population, providing functional evidence for a successful targeting of the tumor-initiating CSC fraction. Depletion of CD133$^+$ cells was observable as early as 5 days after caffeine administration and further enhanced after longer exposure, indicating that prolonged treatment was required for the complete exhaustion of the CD133$^+$ subpopulation, first through the elimination of the rapid cycling cell fraction and consecutively through activation of a slow cycling or even

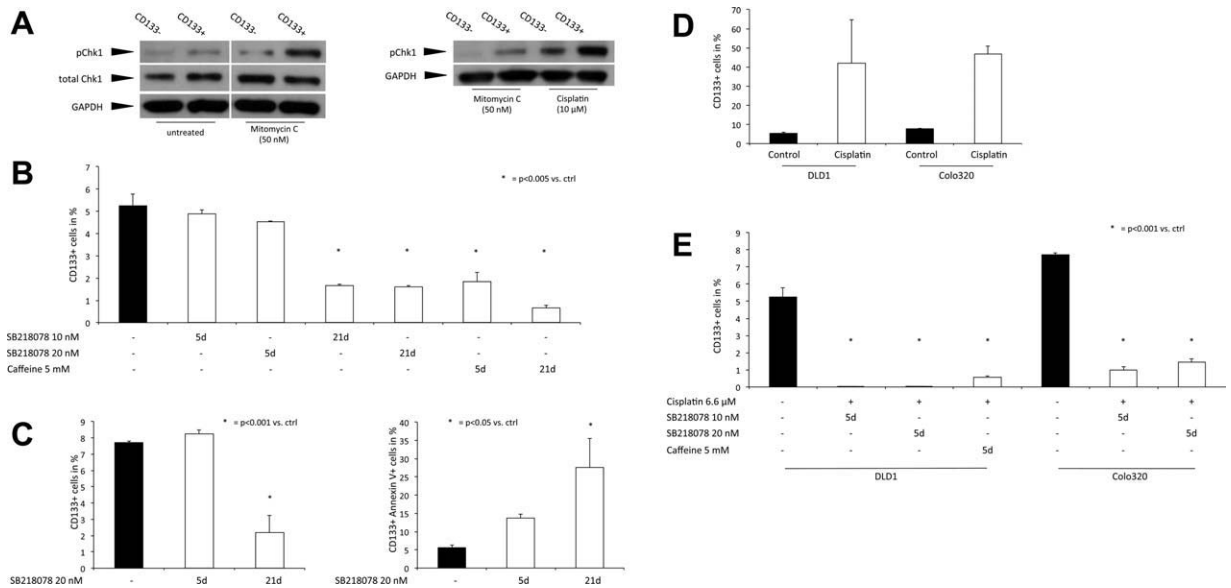

Figure 7. Additive effects of interstrand-crosslinking (ICL)-agents on the depletion of $CD133^+$ cells after inhibition of the ataxia telangiectasia and Rad3 related (ATR)/checkpoint homolog (CHK1) axis. **(A):** Western blotting showing increased Chk1 phosphorylation in $CD133^+$ as compared with $CD133^-$ DLD1 cells on treatment with ICL-agents: Comparison of pCHK1 and CHK1 protein levels in $CD133^+$ and $CD133^-$ cells either left untreated or treated with mitomycin C (left panel), representative results from $n = 2$ experiments are shown. Comparison of pCHK1 protein levels in $CD133^+$ and $CD133^-$ cells treated with either mitomycin C or cisplatin (right panel), representative results from $n = 3$ experiments are shown. **(B):** $CD133^+$ fraction of DLD1 cells after treatment with SB218078 or caffeine for 5 or 21 days, respectively. For illustrative purposes, data for long-term SB218078 treatment were taken from Figure 4E, for caffeine treatment at 5 mM from Figure 2B. **(C):** Total $CD133^+$ cell fraction (left panel) and $CD133^+$ Annexin V^+ subset (right panel) of Colo320 cells after treatment with SB218078 for 5 or 21 days (left panel). **(D):** $CD133^+$ fraction of DLD1 and Colo320 cells after treatment with cisplatin at 6.6 μM for 5 days. **(E):** $CD133^+$ fraction of DLD1 and Colo320 cells after pretreatment with SB218078 or caffeine for 5 days, followed by cisplatin for 2 days. Abbreviation: GAPDH, glyceraldehyde 3-phosphate dehydrogenase.

quiescent fraction. Consistently, caffeine increased the proliferating fraction of $CD133^+$ cells in our experiments.

A panel of small molecule inhibitors was applied to dissect the contributions of the different PIK kinases on the caffeine-induced preferential depletion of $CD133^+$ cells. As no specific ATR-inhibitors are currently available, several potent, but in comparison with the highly specific ATM inhibitors, less-specific inhibitors of CHK1 as the major effector kinase of ATR were used as surrogates for ATR inhibition. In contrast to the ATM inhibitor KU-55399 and the MTOR inhibitor RAD001, only CHK1 inhibitors mimicked the effects of caffeine. As CHK1 activity itself is only marginally suppressed by caffeine [18], whereas the upstream PIK kinase ATR is potently inhibited, these data suggested that the caffeine-induced depletion of $CD133^+$ cells was mediated through direct inhibition of ATR followed by indirect inhibition of its main effector kinase CHK1. Importantly, caffeine exerted its detrimental effects on $CD133^+$ cells already after short-term treatment, whereas the effects of CHK1 inhibitors were observable only after long-term treatment. To exclude different pharmacokinetic properties of the used agents as the underlying reason for the observed differences, our findings were corroborated by a set of siRNA experiments. Consistently, knockdown of CHK1 protein expression over 264 hours did not lead to comparable detrimental effects on the $CD133^+$ cell population as did ATR protein depletion. Furthermore, we analyzed an isogenic FA knockout model [13, 30], as ATR had been linked to the FA DNA-repair pathway [28], but found no evidence for an impact of FA pathway abrogation on the depletion of $CD133^+$ colon cancer cells. Together, these data suggest that besides CHK1 as the major effector kinase of ATR, other ATR-dependent, but FA-independent pathways are operative in this setting.

The complete disruption of the *ATR* gene is a lethal event in human somatic cells [31] and no applicable cellular model presently exists to investigate the null state of the *ATR* gene. However, the hypomorphic *ATR*-inactivating splicing mutation $2101^{A\rightarrow G}$, naturally found in Seckel syndrome patients [32], causes subtotal depletion of ATR protein without gross effects on cancer cell growth or viability [14, 30]. Therefore, cancer cells homozygously harboring this mutation ($ATR^{s/s}$ cells) were used as a highly specific tool to model ATR inhibition in tumors. $ATR^{s/s}$ cells were virtually depleted of $CD133^+$ cells as compared with parental $ATR^{+/+}$ cells. Consistently, $ATR^{s/s}$ cells were impaired in sphere formation capacity and unable to form tumors in vivo. $ATR^{s/s}$ cells did not show significant differences in proliferation rates as compared with their $ATR^{+/+}$ counterparts, excluding that their loss of tumorigenicity was attributable to a hypothetical cell cycle arrest. It should be noted that a limitation of our genetic *ATR* model is that confounding artifacts due to clonal variability cannot definitively be excluded [30]. Therefore, our data require cautious interpretation, especially when considering the CD133 expression status of the originally derived $ATR^{s/s}$ cell clones. As can be derived from our initial experiments, tumorigenicity was mainly restricted to the $CD133^+$ cell fraction of DLD1 colon cancer cells, which constituted only about 5% of the unselected DLD1 cell population. Thus, the engineered $ATR^{s/s}$ cells were more likely originally derived from a $CD133^-$ cell clone, which according to our data, would be expected not to be capable of regenerating tumorigenic $CD133^+$ cells, at least in our short-term experimental setting (14 days). On the other hand, it remains a controversial issue whether non-CSC or a subpopulation of them might be able to regenerate CSC in the long run, or correspondingly, whether $CD133^-$ $ATR^{+/+}$ cells might at some point regenerate $CD133^+$ cells [33]. Taken together,

our data demonstrate that ATR-deficient $CD133^-$ cancer cells retain a nontumorigenic phenotype for at least several months during cell culture.

To exclude potential artifacts due to clonal variability, we employed a third model of ATR function, using RNA-interference through repetitive application of ATR siRNA, which facilitated the continuous depletion of ATR protein in unselected colon cancer cell populations. Similar to the results obtained in the genetic model, we observed a time-dependent decrease of the $CD133^+$ cell fraction in ATR siRNA-treated cells along with a concomitant reduction of the in vivo tumorigenicity of the remaining cell population, strongly indicative of a successful targeting of the tumor-initiating stem cell fraction. In contrast to $ATR^{s/s}$ or caffeine-treated cells, however, ATR siRNA-treated cells did not exhibit a complete abrogation of in vivo tumor formation in all animals. This could most likely be ascribed to an inevitable methodological shortcoming of experiments applying siRNA technology, that is, the incomplete targeting on the cellular level, generally leaving a remaining subpopulation of not efficiently siRNA-transfectable cells (including $CD133^+$ cells), unaffected. Accordingly, traceable amounts of ATR protein were still detectable in the ATR siRNA-treated cell population after 384 hours of repetitive siRNA-application. As a consequence, the decreased, but maybe not absent, tumorigenic cell fraction on ATR siRNA treatment would be expected to lead to a significantly decreased, but not absent, tumor take rate, as observed in our experiments. Interestingly, in those rare instances, in which tumors were generated by ATR siRNA-treated cell populations, these tumors were clearly diminutive as compared with those observed in control mice. This could be explained by the decreased fraction of tumorigenic $CD133^+$ cells in the ATR siRNA-treated population, as a smaller fraction of tumor-initiating cells could perceivably also account for a decreased tumor size in those rare instances of successful tumor formation. Indeed, a very rare occurrence of $CD133^+$ cells was observable in tumors that originated from ATR siRNA-treated cells. Another explanation, consistent with the observed sparse proliferation activity of the diminutive tumors in vivo, would be that these tumors did not arise from the successfully eliminated tumor-initiating cell fraction but rather from an untargeted subset of short-lived transient amplifying cells, which only divide a finite number of times until they become terminally differentiated and finally undergo senescence [34].

A preferential activation of the DDR, comprising both amplified checkpoint activation and increased DNA-repair, has previously been proposed as a likely mechanism of CSC drug-resistance [11, 12] and could also explain the increased sensitivity of $CD133^+$ colon cancer cells toward ATR inhibition; ATR is a central regulator of the replication checkpoint, which blocks cell cycle progression on detection of endogenous or exogenously induced SRF. In this process, ATR stabilizes SRF via its main effector kinase CHK1 and prevents the inappropriate processing of DNA [29]. Accordingly, cells harboring a complete disruption of the *ATR* gene display increased chromosome breaks even in the absence of exogenous replication stress, most likely induced through SRF occurring during normal cellular proliferation, and are not viable over extended periods of time [31]. The significantly stronger upregulation of CHK1 phosphorylation in the $CD133^+$ as compared with the $CD133^-$ cell fraction on treatment with SRF-inducing ICL-agents in our experiments thus supports a preferential activation of the ATR-dependent DDR also in colon CSC.

Consistently, treatment with SRF-inducing ICL-agents accelerated the depletion of $CD133^+$ cells on ATR inhibition, further supporting that the detrimental effects of caffeine specifically on $CD133^+$ cells were attributable to the particularly reduced capability of these cells to repair, endogenously or exogenously inflicted, SRF when ATR function was impaired. It is tempting to speculate that the impaired DNA repair capability of $CD133^+$ cells in response to ATR inhibition could be ascribed structurally to differences in chromatin compaction between $CD133^+$ and $CD133^-$ cells. Overall, chromatin accessibility, a dynamic process largely mediated by chromatin compaction, represents an innate property of stem cells, which is lost during differentiation [35]. The degree of chromatin compaction, on the other hand, determines at least in part the extent of DNA damage, the feasibility of DNA repair [36], and the strength of the DDR [37] and could thus explain a particularly strong dependence of CSC on an intact DDR.

On confrontation with DNA damage, the DDR mediates whether cells undergo a replication arrest to allow DNA repair, bypass the DNA damage and continue to replicate DNA, or eventually, undergo apoptosis [38]. We found that after caffeine treatment, apoptotic cell death did not occur immediately in $CD133^+$ cells, but progressively increased with cumulative BrdU incorporation, excluding cytotoxicity as the sole source of the caffeine-induced effects. Notably, a small fraction of $AnnexinV^+$ $CD133^+$ cells was detectable up to 168 hours after treatment initiation, likely representing the CSC fraction progressively recruited to enter an active cell cycle. Consistently, after an initial caffeine-induced increase of $CD133^+$ $AnnexinV^+$ cells, their amount subsequently declined, paralleling the decline of total $CD133^+$ cell numbers. Thus, the caffeine-induced depletion of $CD133^+$ cells was at least in part attributable to proliferation-dependent induction of apoptosis. As apoptosis was triggered by caspase 8 and reinforced by a mitochondrial amplification loop involving the recruitment of caspase 9, sensitization to extrinsic receptor-mediated apoptosis might provide another tool for the specific depletion of the CSC fraction in colon cancer.

Conclusion

Using three independent model systems, that is, pharmacological ATR inhibition, genetic inactivation of the *ATR* gene, and RNA interference-mediated ATR protein depletion, we found that inhibition of ATR function depleted the tumorigenic $CD133^+$ cell fraction of established human colon cancer cell lines as well as xenograft-derived primary colon cancer cells. This effect was attributable at least in part to apoptosis, accelerated on cotreatment with common chemotherapeutics that generate SRF, and accompanied by a drastically decreased in vitro and in vivo tumorigenicity of the remaining cells. Mechanistically, the preferential depletion of tumorigenic $CD133^+$ cells was attributable to the preferential activation of the ATR-dependent DDR in these cells. Our study thus illustrates a novel approach to selectively eliminate the tumorigenic cell population in colon cancer. As the caffeine blood levels required for inhibiting ATR function cannot be achieved in vivo due to the narrow therapeutic window and the pronounced cardiovascular side effects of caffeine and its derivatives, our study provides a strong rationale for the pharmaceutical development of specific ATR inhibitors as a potentially powerful approach to eliminate CSC in colorectal cancer [39–41].

Acknowledgments

We thank Sonia Alcalá, Aurora Garcia, Martin Luckner, and Karin Nispel for excellent technical assistance. This work was

supported by grants to E.G. (DFG Ga762/3-1, Bavarian Academy of Sciences and Arts, Förderprogramm für Forschung und Lehre #544, Friedrich-Baur-Foundation, K. L. Weigand trust) and C.H. (Krebshilfe 108168, BaCaTeC, Friedrich-Baur-Foundation, ERC Advanced Investigator Grant Pa-CSC 233460).

Disclosure of Potential Conflicts of Interest

The authors indicate no potential conflicts of interest.

References

1 Reya T, Morrison SJ, Clarke MF et al. Stem cells, cancer, and cancer stem cells. Nature 2001;414:105–111.
2 Brabletz T, Jung A, Spaderna S et al. Opinion: Migrating cancer stem cells—An integrated concept of malignant tumour progression. Nat Rev Cancer 2005;5:744–749.
3 Hermann P, Huber S, Herrler T et al. Distinct populations of cancer stem cells determine tumor growth and metastatic activity in human pancreatic cancer. Cell Stem Cell 2007;1:313–323.
4 O'Brien CA, Pollett A, Gallinger S et al. A human colon cancer cell capable of initiating tumour growth in immunodeficient mice. Nature 2007;445:106–110.
5 Ricci-Vitiani L, Lombardi D, Pilozzi E et al. Identification and expansion of human colon-cancer-initiating cells. Nature 2007;445:111–115.
6 Mueller MT, Hermann PC, Witthauer J et al. Combined targeted treatment to eliminate tumorigenic cancer stem cells in human pancreatic cancer. Gastroenterology 2009;137:1102–1113.
7 Todaro M, Alea MP, Di Stefano AB et al. Colon cancer stem cells dictate tumor growth and resist cell death by production of interleukin-4. Cell Stem Cell 2007;1:389–402.
8 Dylla SJ, Beviglia L, Park IK et al. Colorectal cancer stem cells are enriched in xenogeneic tumors following chemotherapy. Plos One 2008;3:e2428.
9 Bucher N, Britten CD. G2 checkpoint abrogation and checkpoint kinase-1 targeting in the treatment of cancer. Br J Cancer 2008;98:523–528.
10 Ashwell S, Zabludoff S. DNA damage detection and repair pathways—Recent advances with inhibitors of checkpoint kinases in cancer therapy. Clin Cancer Res 2008;14:4032–4037.
11 Bao S, Wu Q, Mclendon R et al. Glioma stem cells promote radioresistance by preferential activation of the DNA damage response. Nature 2006;444:756–760.
12 Eyler CE, Rich JN. Survival of the fittest: Cancer stem cells in therapeutic resistance and angiogenesis. J Clin Oncol 2008;26:2839–2845.
13 Gallmeier E, Calhoun ES, Rago C et al. Targeted disruption of FANCC and FANCG in human cancer provides a preclinical model for specific therapeutic options. Gastroenterology 2006;130:2145–2154.
14 Hurley PJ, Wilsker D, Bunz F. Human cancer cells require ATR for cell cycle progression following exposure to ionizing radiation. Oncogene 2007;26:2535–2542.
15 Jimeno A, Feldmann G, Suarez-Gauthier A et al. A direct pancreatic cancer xenograft model as a platform for cancer stem cell therapeutic development. Mol Cancer Ther 2009;8:310–314.
16 Dalerba P, Dylla SJ, Park IK et al. Phenotypic characterization of human colorectal cancer stem cells. Proc Natl Acad Sci USA 2007; 104:10158–10163.
17 Lavrik IN, Golks A, Krammer PH. Caspases: Pharmacological manipulation of cell death. J Clin Invest 2005;115:2665–2672.
18 Sarkaria JN, Busby EC, Tibbetts RS et al. Inhibition of ATM and ATR kinase activities by the radiosensitizing agent, caffeine. Cancer Res 1999;59:4375–4382.
19 Hickson I, Zhao Y, Richardson CJ et al. Identification and characterization of a novel and specific inhibitor of the ataxia-telangiectasia mutated kinase ATM. Cancer Res 2004;64:9152–9159.
20 Huang S, Bjornsti MA, Houghton PJ. Rapamycins: Mechanism of action and cellular resistance. Cancer Biol Ther 2003;2:222–232.
21 Graves PR, Yu L, Schwarz JK et al. The Chk1 protein kinase and the Cdc25C regulatory pathways are targets of the anticancer agent UCN-01. J Biol Chem 2000;275:5600–5605.
22 Ruegg UT, Burgess GM. Staurosporine, K-252 and UCN-01: Potent but nonspecific inhibitors of protein kinases. Trends Pharmacol Sci 1989;10:218–220.
23 Busby EC, Leistritz DF, Abraham RT et al. The radiosensitizing agent 7-hydroxystaurosporine (UCN-01) inhibits the DNA damage checkpoint kinase hChk1. Cancer Res 2000;60:2108–2112.
24 Zhao B, Bower MJ, McDevitt PJ et al. Structural basis for Chk1 inhibition by UCN-01. J Biol Chem 2002;277:46609–46615.
25 Jackson JR, Gilmartin A, Imburgia C et al. An indolocarbazole inhibitor of human checkpoint kinase (Chk1) abrogates cell cycle arrest caused by DNA damage. Cancer Res 2000;60:566–572.
26 Kawabe T. G2 checkpoint abrogators as anticancer drugs. Mol Cancer Ther 2004;3:513–519.
27 Gallmeier E, Hucl T, Calhoun ES et al. Gene-specific selection against experimental Fanconi anemia gene inactivation in human cancer. Cancer Biol Ther 2007;6:654–660.
28 Andreassen PR, D'Andrea AD, Taniguchi T. ATR couples FANCD2 monoubiquitination to the DNA-damage response. Genes Dev 2004; 18:1958–1963.
29 Paulsen RD, Cimprich KA. The ATR pathway: Fine-tuning the fork. DNA Repair (Amst) 2007;6:953–966.
30 Gallmeier E, Kern SE. Targeting Fanconi anemia/BRCA2 pathway defects in cancer: The significance of preclinical pharmacogenomic models. Clin Cancer Res 2007;13:4–10.
31 Cortez D, Guntuku S, Qin J et al. ATR and ATRIP: Partners in checkpoint signaling. Science 2001;294:1713–1716.
32 O'Driscoll M, Ruiz-Perez VL, Woods CG et al. A splicing mutation affecting expression of ataxia-telangiectasia and Rad3-related protein (ATR) results in Seckel syndrome. Nat Genet 2003;33:497–501.
33 Chen R, Nishimura MC, Bumbaca SM et al. A hierarchy of self-renewing tumor-initiating cell types in glioblastoma. Cancer cell 2010; 17:362–375.
34 Barker N, Ridgway RA, van Es JH et al. Crypt stem cells as the cells-of-origin of intestinal cancer. Nature 2009;457:608–611.
35 Meshorer E, Yellajoshula D, George E et al. Hyperdynamic plasticity of chromatin proteins in pluripotent embryonic stem cells. Dev Cell 2006;10:105–116.
36 Cohn MA, D'Andrea AD. Chromatin recruitment of DNA repair proteins: Lessons from the Fanconi anemia and double-strand break repair pathways. Mol Cell 2008;32:306–312.
37 Murga M, Jaco I, Fan Y et al. Global chromatin compaction limits the strength of the DNA damage response. J Cell Biol 2007;178: 1101–1108.
38 Harper JW, Elledge SJ. The DNA damage response: Ten years after. Mol Cell 2007;28:739–745.
39 Nghiem P, Park PK, Kim Y et al. ATR inhibition selectively sensitizes G1 checkpoint-deficient cells to lethal premature chromatin condensation. Proc Natl Acad Sci USA 2001;98:9092–9097.
40 Collis SJ, Swartz MJ, Nelson WG et al. Enhanced radiation and chemotherapy-mediated cell killing of human cancer cells by small inhibitory RNA silencing of DNA repair factors. Cancer Res 2003;63: 1550–1554.
41 Wilsker D, Bunz F. Loss of ataxia telangiectasia mutated- and Rad3-related function potentiates the effects of chemotherapeutic drugs on cancer cell survival. Mol Cancer Ther 2007;6:1406–1413.

See www.StemCells.com for supporting information available online.